Journal of Molecular Histology (2021) 52:1155–1164
https://doi.org/10.1007/s10735-021-10008-y

ORIGINAL PAPER

SDF-1 secreted by mesenchymal stem cells promotes the migration of endothelial progenitor cells via CXCR4/PI3K/AKT pathway

Xiaoyi Wang[1,2] · Huijiao Jiang[2] · Lijiao Guo[2] · Sibo Wang[2] · Wenzhe Cheng[2] · Longfei Wan[2] · Zhongzhou Zhang[2] · Lihang Xing[2] · Qing Zhou[2] · Xiongfeng Yang[2] · Huanhuan Han[2] · Xueling Chen[4] · Xiangwei Wu[2,3]

Received: 13 October 2020 / Accepted: 7 August 2021 / Published online: 12 October 2021

Abstract

Cell-based therapeutics bring great hope in areas of unmet medical needs. Mesenchymal stem cells (MSCs) have been suggested to facilitate neovascularization mainly by paracrine action. Endothelial progenitor cells (EPCs) can migrate to ischemic sites and participate in angiogenesis. The combination cell therapy that includes MSCs and EPCs has a favorable effect on ischemic limbs. However, the mechanism of combination cell therapy remains unclear. Herein, we investigate whether stromal cell-derived factor (SDF)-1 secreted by MSCs contributes to EPC migration to ischemic sites via CXCR4/Phosphoinositide 3-Kinases (PI3K)/protein kinase B (termed as AKT) signaling pathway. First, by a "dual-administration" approach, intramuscular MSC injections were supplemented with intravenous Qdot® 525 labeled-EPC injections in the mouse model of hind limb ischemia. Then, the mechanism of MSC effect on EPC migration was detected by the transwell system, tube-like structure formation assays, western blot assays in vitro. Results showed that the combination delivery of MSCs and EPCs enhanced the incorporation of EPCs into the vasculature and increased the capillary density in mouse ischemic hind limb. The numbers of CXCR4-positive EPCs increased after incubation with MSC-conditioned medium (CM). MSCs contributed to EPC migration and tube-like structure formation, both of which were suppressed by AMD3100 and wortmannin. Phospho-AKT induced by MSC-CM was attenuated when EPCs were pretreated with AMD3100 and wortmannin. In conclusion, we confirmed that MSCs contributes to EPC migration, which is mediated via CXCR4/PI3K/AKT signaling pathway.

Keywords Mesenchymal stem cells · Endothelial progenitor cells · Stromal cell-derived factor-1 · CXCR4 · AKT · Mouse model of hind limb ischemia

Introduction

Organisms require blood vessels to carry oxygen and nutrients for proper development and physiological functioning, abnormalities in this process may lead to disease development or progression. Tissue ischemia, which is characterized as an insufficient supply of oxygen and nutrients, impairs bodily function and can even be life-threatening (Couffinhal et al. 1998). Naturally, neovascularization is required to maintain the integrity and function of ischemic tissues.

Currently, therapeutic neovascularization based on stem cells is under intense investigation. A combination cell therapy that includes EPCs and MSCs improves perfusion in patients with severe ischemic limbs (Lasala et al. 2010, 2011, 2012). However, the underlying mechanisms are poorly understood. A number of researchers have focused on SDF-1 and its receptor CXCR4 as critical regulators of stem cell recruitment (Ghadge et al. 2011; Yu et al. 2015; Tsai

Xiaoyi Wang, Huijiao Jiang and Lijiao Guo have contributed equally to this work.

✉ Xueling Chen
chenxueling@shzu.cn

✉ Xiangwei Wu
wxwshz@126.com

[1] Department of Pediatric Hematology and Oncology, The First Affiliated Hospital of Zhengzhou University, No. 1 Jianshe East Road, Zhengzhou 450052, Henan, China

[2] Laboratory of Translational Medicine, Medical School of Shihezi University, No. 59 North 2 Road, Shihezi 832002, Xinjiang, China

[3] Department of General Surgery, The First Affiliated Hospital of Shihezi University, No. 107 North 2 Road, Shihezi 832008, Xinjiang, China

[4] Department of Immunology, Medical School of Shihezi University, No. 59 North 2 Road, Shihezi 832002, Xinjiang, China

et al. 2014). Furthermore, cell migration is mediated through the activation of PI3K/AKT, which is a major downstream pathway of SDF-1/CXCR4 (Xiu et al. 2020). MSCs secrete a vast array of chemoattractants, such as SDF-1, vascular endothelial growth factor, platelet-derived growth factor, hepatocyte growth factor, insulin-like growth factor-1, fibroblast growth factor, and hypoxia inducible factor-1α (Vanden 2014). Studies suggest that the paracrine property of MSCs plays a greater role in therapeutic angiogenesis than their transdifferentiation or cell infusion (Yong et al. 2018). In view of the reasons stated above, we speculate that AKT protein is phosphorylated by PI3K when SDF-1 secreted by MSCs engages the corresponding receptor CXCR4 on EPC surface, which induces EPC migration.

Given the above, we investigated whether a combination cell therapy that includes EPCs and MSCs improves perfusion in the mouse model of hind limb ischemia. We performed in vitro experiments to explore the potential molecular mechanisms involved in EPC migration. An excellent understanding of the mechanisms involved in the effect of cytokines secreted by MSCs on EPC migration will contribute to maximizing the local concentration of EPCs in the ischemic area and increase cell invasion. This information will provide insights into effective therapeutic approaches for cellular transplantation.

Materials and methods

Mice

C57BL/6 mice that respectively were 1–2 (15–25 g) and 6–7 (25–30 g) months old were obtained from the Laboratory Animal Center of Xinjiang Medical University (Urumqi, China). Mice were maintained under a 12 h light/dark cycle in a constant temperature and humidity environment, food and water were available ad libitum. All experiments were approved by the Shihezi University Ethics Committee (Shihezi, China) and performed in accordance with the Xinjiang Medical University Guide for Laboratory Animals.

Cell isolation and culture

MSCs and EPCs derived from murine bone marrow were simultaneously isolated as previously described (Wang et al. 2018). MSCs were cultured in complete Dulbecco's modified Eagle's medium (DMEM) that consisted of low-glucose DMEM (Gibco; Thermo Fisher Scientific, Waltham, MA, USA), 10% fetal bovine serum (FBS; Hyclone, GE Healthcare Life Sciences, Logan, UT, USA), 100 U/ml penicillin, and 100 U/ml streptomycin (both from Sigma-Aldrich; Merck KGaA, Darmstadt, Germany). EPCs were cultured in endothelial growth medium (EGM) that contained endothelial cell basal medium-2, EGM™-2 MV SingleQuots™ (both from Lonza Group, Basel, Switzerland), 100 U/ml penicillin, and 100 U/ml streptomycin. Both were maintained at 37 °C in a humidified 5% CO_2 incubator. When the cells reached 80–90% confluence, the cultures were harvested using StemPro Accutase (Gibco; Thermo Fisher Scientific). Passage 3 MSCs and late EPCs cultured for more than 14 days were used for cell transplantation.

Unilateral hind limb ischemia (HLI) model and cell transplantation

The femoral arteries of 6-month-old (30–35 g) male mice were ligated to induce left hind limb ischemia as described previously (Niiyama et al. 2009). To track EPC incorporation at early time point after transplantation (on day 3), late EPCs were labeled using the Qtracker® 525 Cell Labeling Kit (Life technology, Carlsbad, CA, USA) according to the manufacturer's protocol. At 24 h after operation, the mice with ischemic limbs were randomly allocated into four groups as follows: phosphate-buffered saline (PBS) group; MSC (1×10^6) group; Qdot® 525 labeled-EPCs (1×10^6) group; and a combination of MSCs (1×10^6) and Qdot® 525 labeled-EPCs (1×10^6) group. Cells or PBS were administrated as above. After 3 days, the adductor muscles of ischemic and healthy limbs were immediately harvested for frozen section samples.

We also investigated the combination effect of MSCs and EPCs on neovascularization at late time point after transplantation (on day 14). At 24 h after operation, the mice were randomly allocated into four groups that received the following injections: PBS; MSCs (1×10^6); EPCs (1×10^6); or a combination of MSCs (1×10^6) and EPCs (1×10^6). MSCs suspended in 50 µl of PBS or PBS alone were infused to the gracilis muscles at four sites. Then, EPCs suspended in 20 µl of PBS or PBS alone were injected via the tail vein. After 14 days, the adductor muscles of ischemic and healthy limbs were harvested for paraffin section samples.

Morphologic observation and histological assessment of transplanted mice

It was well known that blood circulation disorder resulted in necrosis. To visually characterize morphological changes, the limb salvage, toe loss, and foot necrosis of ischemic hind limbs were recorded when mice were subjected to the femoral artery ligation for 14 days.

For frozen section samples, tissues were embedded in OCT compound and snap frozen in liquid nitrogen. Frozen sections with a thickness of 8 µm were mounted on silane-coated glass slides and air-dried for 1 h. The section samples were then washed for 5 min thrice with PBS and blocked with normal goat serum (Solarbio, Beijing, China)

for 20 min at room temperature (RT). Subsequently, the sections were stained with rabbit antibody against mouse CD31 (1:100; Cell Signaling Technology, Danvers, MA, USA) overnight at 4 °C. After three washes in PBS for a total of 30 min, a secondary TRITC-conjugated goat anti-rabbit IgG antibody (1:50; ZSGB-BIO, Beijing, China) was added for 30 min at RT. Any excess liquid was removed from the specimen, and one drop of the mounting reagent (glycerinum: PBS = 9:1) was applied (Thermo Fisher Scientific) to the specimens. Photographs were taken using a Zeiss LSM 510 META laser confocal microscope (Zeiss, Germany).

For paraffin section samples, tissues were fixed, dehydrated, and paraffin embedded. Paraffin sections with a thickness of 5 μm were prepared. Vascular density was determined by quantifying the CD31-positive vessels/mm^2 present in the peri-infarct region. The sections were incubated with primary rabbit anti-mouse CD31 (1:200; Abcam) and then with secondary horseradish peroxidase (HRP)-conjugated goat anti-rabbit antibody (1:10,000; Abcam). After rinsing with PBS thrice, a DAB working solution was added for 5 min. The sections were counterstained with hematoxylin for 10 s and mounted with neutral balsam. Photographs were taken using an inverted microscope (Olympus, Japan). CD31-positive staining was measured in two sections of four distinct views of each specimen by using the Image-Pro Plus 6.0 software.

Preparation of MSC-CM

MSCs were seeded in DMEM supplemented with 10% FBS until 90% confluence. After washing the cells with PBS, the medium was changed into EBM supplemented with 1% BSA and conditioned at 37 °C and 5% CO_2. After 24 and 48 h, the medium was collected and centrifuged at 300 g for 10 min to remove cell debris and then filtered (0.22 μm pore size; Merck Millipore, Billerica, MA, USA). The control medium was comprised of EBM and 1% BSA in the absence of cell procedure.

Flow cytometry analysis of CXCR4 expression on EPCs induced by MSC-CM

We investigated whether SDF-1 secreted by MSCs affected CXCR4 expression in EPCs. First, quantitative immunoassays were used to assess the ability of MSCs to produce SDF-1 according to the manufacturer's protocol (Elabscience, Wuhan, China). The MSC-CM obtained above was detected. Data were acquired using a spectrophotometer, and measurement wavelength was 450 nm.

CXCR4 expression in EPCs was measured via flow cytometry. EPCs were cultured with EGM until 90% confluence. After serum-free starvation overnight, EPCs were divided into four groups and cultured with EBM + 2% FBS, MSC-CM + 2% FBS for 24 h, MSC-CM + 2% FBS for 48 h, and MSC-CM + 2% FBS for 72 h. Then, EPCs were harvested and incubated with rabbit anti-mouse CXCR4 antibody (Abcam) for 30 min at RT, washed with PBS thrice, and incubated with TRITC-conjugated goat anti-rabbit IgG at 4 °C in the dark. Data were acquired using a flow cytometer (Becton Dickinson, USA).

Migration assays

To investigate the effect of cytokines secreted by MSCs on EPC migration through CXCR4/PI3K/AKT signaling pathway, we performed the assays using the transwell assembly (Corning) with 6.5 mm diameter inserts (8 μm pore size) as described previously (Li et al. 2018). Briefly, EPCs were pretreated with 50 ng/ml AMD3100 for 2 h (Tsai et al. 2014) and 0.1 μM wortmannin for 1 h (Teranishi et al. 2009). AMD3100 is a highly selective antagonist of SDF-1 that binds to its receptor CXCR4. By comparison, wortmannin is a PI3K inhibitor. Non-pretreated EPCs and pretreated EPCs (1×10^5) were harvested and suspended in 100 μl of EBM-2 supplemented with 2% FBS and then reseeded in the upper compartment. MSCs (5×10^4) were suspended in 600 μl EBM-2 supplemented with 2% FBS and replated in the lower compartment of the transwell chambers. After incubation at 37 °C for 18 h, the cells on the filters were stained with 0.1% crystal violet. Thereafter, the filters were washed with 33% acetic acid, and the OD_{570} nm value of the eluate was detected using a spectrophotometer (Thermo Fisher Scientific).

Tube-like structure formation assays

The tubule formation assays were performed with a thick Matrigel (BD Biosciences) according to the manufacturer's instruction. Briefly, a pre-cooled 48-well plate was coated with the Matrigel, which was melted into liquid at 4 °C overnight. The plate was placed at 37 °C and 5% CO_2 for 45 min to allow polymerization of the Matrigel. Meanwhile, EPCs were pretreated with 50 ng/ml AMD3100 for 2 h and 0.1 μM wortmannin for 1 h. The nonpretreated EPCs and pretreated EPCs (2×10^4) were suspended in 350 μl of MSC-CM or EBM supplemented with 2% FBS and then inoculated on top of the Matrigel. After incubating for 6–8 h at 37 °C and 5% CO_2, all wells were photographed (×5 amplification) using an inverted microscope (Zeiss). Tubule formation was quantified with the Angiogenesis analyzer from Image-Pro Plus 6.0.

Western blotting

To investigate the migration signaling, we pre-incubated EPCs with 50 ng/ml AMD3100 for 2 h or 0.1 μM

wortmannin for 1 h. The EPCs were then incubated for 30 min or 48 h with MSC-CM + 5% FBS. Cells were harvested for immunoblotting of phospho-AKT, total AKT, Girdin, Paxillin and PAK1, the last three proteins of which correlated with cell migration. Extracts were prepared using a lysis buffer solution (RIPA:PMSF:protein phosphatase inhibitor = 100:1:1; Solarbio). Proteins were measured using the Pierce™ BCA protein assay kit (Pierce; Thermo Scientific) with BSA as a standard. Equal amounts of proteins (20 μg) were separated in 10% sodium dodecyl sulfate–polyacrylamide gel electrophoresis and transferred to nitrocellulose membranes (Amersham Biosciences). The membranes were then blocked with 5% nonfat dried milk in Tween phosphate-buffered saline (T-PBS) and probed with rabbit polyclonal anti-phospho-AKT (1:2000; Cell Signaling Technology), total AKT (1:2000; Cell Signaling Technology), Girdin (1:1000; Abcam), Paxillin (1:5000; Abcam) and PAK1 (1:1000; Abcam) antibody overnight at 4 °C. After incubation with primary antibody, blots were washed thrice in T-PBS and incubated for 1 h with anti-rabbit HRP-conjugated IgG (1:10,000; Abcam). The protein bands were detected by Odyssey CLx system (Gene Company Limited, Hong Kong, China), and the intensities of the immunoblot bands were quantified using the Odyssey CLx Image Studio 3.1. Immunoblots were re-probed with rabbit anti-mouse β-actin (Abcam) for normalization. After digitization, band intensities were evaluated with GraphPad Prism 5 (GraphPad Software, CA, USA).

Statistical analysis

All values were expressed as mean ± standard deviations of the mean. Comparisons between two groups were analyzed using an independent t-test, one-way ANOVA was used to compare the differences among three groups and more. Statistical analysis was performed using GraphPad Prism 6.0, and p value < 0.05 was considered statistically significant.

Results

Contribution of MSCs to EPC incorporation into ischemic hind limb neovasculature

To study the effect of MSCs on recruitment of EPCs from the systemic circulation, we measured the incorporation of injected EPCs into the microvasculature in the ischemic hind limb. Transplanted EPCs labeled with Q-tracker were identified in tissue sections by green fluorescence, whereas the native mouse vasculature stained by anti-CD31 antibody was identified by red fluorescence in the same tissue sections. 3 days after cell administration, the incorporation of EPCs into vasculature increased in the combined group compared with that in the EPC group alone (Fig. 1a), which was confirmed via statistical analysis (Fig. 1b).

Local delivery of MSCs increase vascular ratio per area

Angiogenesis promoted by MSCs results from the paracrine effect, hence, we evaluated its beneficial effect with the combined cell therapy. At 14 days subjected to the femoral artery ligation, morphologic observation showed the mice receiving the combined injection of MSCs and EPCs underwent toenail salvage compared with PBS injection and the single cell injection (Fig. 2a). Statistically speaking, the numbers of limb salvage, toe loss and toe necrosis had not siginificant difference in four groups. However, toenail necrosis numbers in the combination groups of MSCs and EPCs markedly diminished compared with those in PBS groups (Table 1), suggesting that the combined cell therapy was conducive to angiogenesis.

It was known that the nuclei of muscle cells were on the edge, and they moved inward when muscle cells degenerated. At 14 days after cell delivery, hematoxylin and eosin (HE) staining showed that a small number of nuclei were located in the center of muscle cells in the combination groups of MSCs and EPCs in contrast to the control groups and the single cell treatment groups (Fig. 2b).

The vascular ratio per area was represented by CD31-positive staining (Fig. 2b). It was significantly higher in the combined groups than in the control groups and the single cell treatment groups (Fig. 2c).

SDF-1 production by MSCs and CXCR4 expression by EPCs

After 24 h, 48 h and 72 h, SDF-1 secreted by MSCs was 0.62, 2.61 and 1.93 ng/ml, respectively (Fig. 3a). Therefore, MSC-CM was collected from MSCs cultured for 48 h.

CXCR4 was measured via flow cytometry when EPCs were incubated by MSC-CM with 5% FBS. Results showed that the rate of CXCR4-positive EPCs was 50.3%, 67.6%, and 51.9% after 24, 48, and 72 h, respectively. By contrast, the rate of CXCR4-positive EPCs was 27.7% when cultured in EBM with 5% FBS (Fig. 3b). Statistically, the protein level of CXCR4 in EPCs significantly increased after incubation with MSC-CM (Fig. 3c).

Effect of SDF-1 secreted by MSCs on EPC migration

EPC migration is a critical step in neovascularization. Transwell migration assays revealed that EPCs, which migrated to the lower surface of the inserts, significantly increased in the MSC-CM groups compared with the EBM groups. We examined the mechanism of SDF-1 secreted

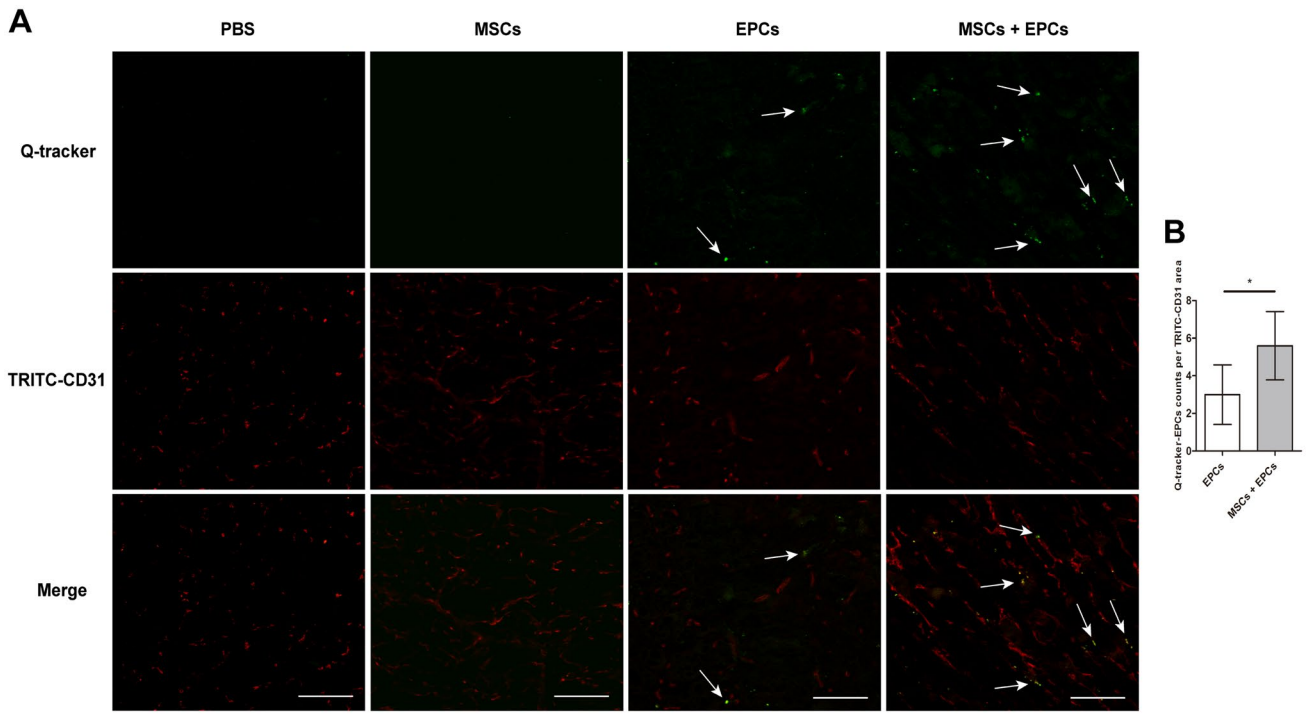

Fig. 1 Representative photomicrographs of EPC incorporation into neovasculature sites in vivo. **a** The top, middle, and bottom panels showed Q-tracker-labeled EPCs (green, indicated by arrows) between the skeletal myocytes, CD31-positive vasculature (red), and EPC incorporation into vasculature (yellow, indicated by arrows), for 3 days after administration (n = 3). Scale bar, 100 μm. **b** The statistical analysis of the incorporation of EPCs into vasculature in the EPC groups alone and the MSC + EPC groups. $^{*}p < 0.05$

by MSCs on EPC migration with AMD3100 and wortmannin. Notably, the pre-incubation of AMD3100 or wortmannin significantly lessen EPC migration (Fig. 3d, e). The results demonstrated that blockade of CXCR4 remarkably suppressed EPC migration induced by MSCs, which was similar to the blockade of PI3K.

Effect of SDF-1 in MSC-CM on tube-like structure formation of EPCs

Cell migration was also included in the process of tube-like structure formation. Compared with EBM, EPCs were prone to migrate, assemble, and form complete tube-like structures under MSC-CM induction. The pre-incubation of AMD3100 or wortmannin resulted in incomplete tubule formation than that seen in no pre-incubation group containing MSC-CM (Fig. 3f). These structures were quantified with total mesh area and total segment length. The data indicated that the numbers of total mesh area and total segment length significantly decreased with AMD3100 or wortmannin pre-incubation (Fig. 3g). The blockade of CXCR4 had been suggested to suppress the formation of a tube-like structure, which was similar to the blockade of PI3K.

Effect of SDF-1 in MSC-CM on AKT phosphorylation in EPCs

To investigate whether SDF-1 in MSC-CM affects AKT phosphorylation, we evaluated AKT Ser473 phosphorylation in EPCs stimulated with MSC-CM for 30 min. Western blot analysis revealed that MSC-CM incubation remarkably increased the level of phospho-AKT, as well as Girdin, Paxillin and PAK1 in EPCs, however, the increase was significantly suppressed by AMD3100 or wortmannin (Fig. 4a, b).

Discussion

The therapeutic approach of combined MSCs and EPCs stems from the evidence that the process of angiogenesis may need more than one cytokine or cell type to optimize new vessel formation. EPCs might be fundamentally used to refer to populations of cells that are capable of differentiation into mature endothelial cells, with purportedly physiological roles in neovascularization (Chong et al. 2016). Several clinical and preclinical studies have documented that administrated EPCs successfully augment neovascularization in multiple animal models of vascular injury (Sun et al. 2011; Xue et al. 2020). An important challenge for therapeutic

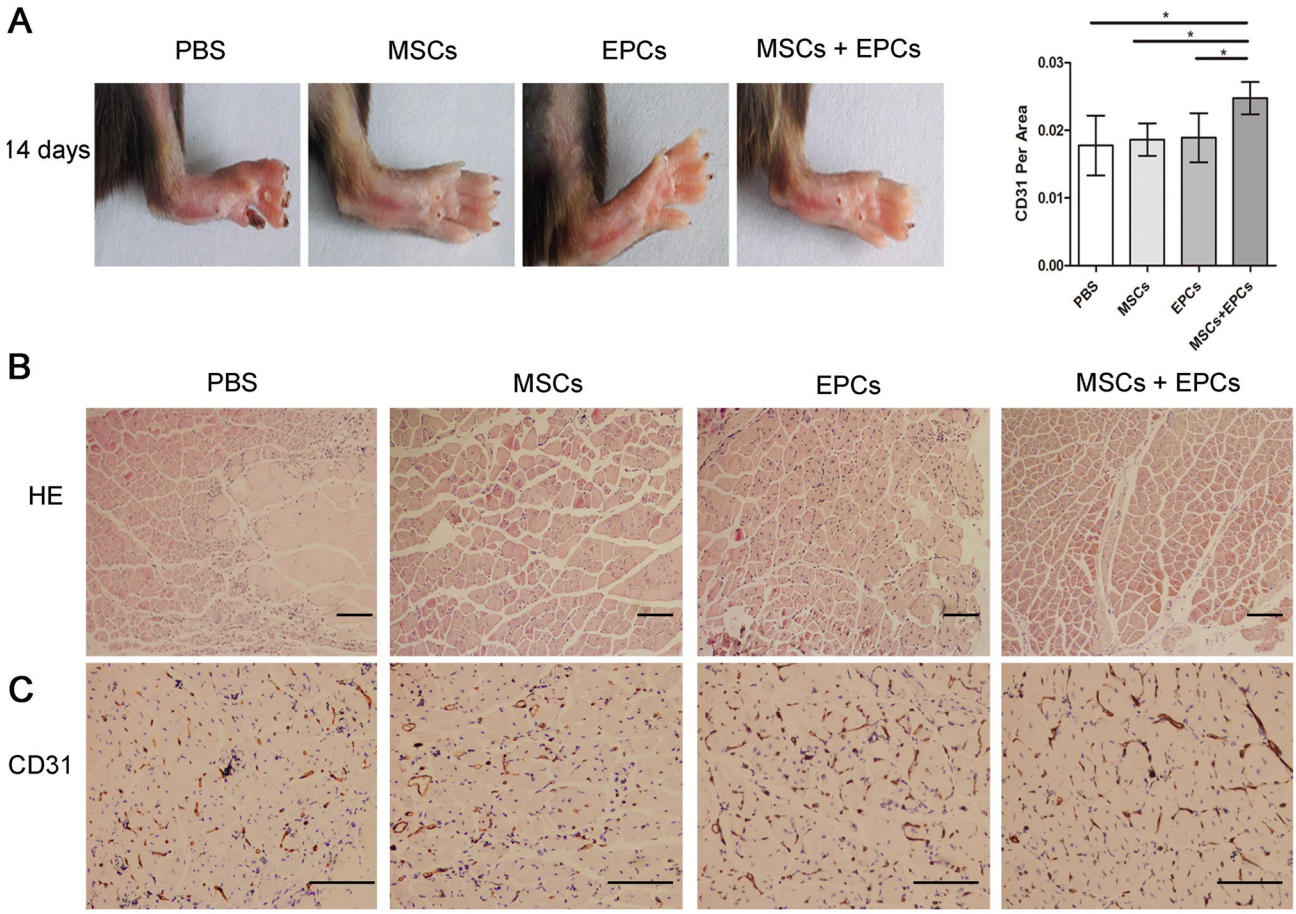

Fig. 2 Morphologic observation and histological analysis of mice ischemic hind limb. **a** Toes appearance were observed on 14 days after femoral artery ligation. **b** Morphological characteristics of skeletal muscle cells and capillary counts were identified by HE staining in top panels and CD31 immunohistochemistry in bottom panels, respectively (n = 3). Scale bar, 100 μm. **c** Quantification analysis of vascular ratio per area. *$p < 0.05$

Table 1 the quantitative results for limb salvage, toe loss, and foot necrosis in different groups

	PBS (n = 4)	MSCs (n = 7)	EPCs (n = 4)	MSCs + EPCs (n = 7)
Limb salvage	3/n	7/n	3/n	5/n
Toe loss	1/5n	0/5n	0/5n	0/5n
Toe necrosis	4/5n	3/5n	1/5n	2/5n
Toenail necrosis	9/5n	12/5n	6/5n	6/5n**

[n]the number of mice, [5n]the number of mice toe/toenail

**$p < 0.01$

neovascularization is the migration of a sufficient number of EPCs to the injury site to participate in neovascularization. EPCs cultured in vitro are distinguished into early and late EPCs depending on their time of appearance in culture (Medina et al. 2017). In the present study, we used late EPCs to identify their integration into endothelium because early EPCs generate high levels of angiogenic cytokines, and late EPCs have the potential to form blood vessels (Barsotti et al. 2009).

MSCs are non-hemopoietic stromal cells, which are characterized by the multilineage differentiation potential, paracrine action, and low immunogenicity. MSCs make an important contribution to postnatal vasculogenesis, especially during tissue ischemia (Han et al. 2019). Mounting evidence shows that paracrine action probably underlies the vascular effects of MSCs (Konoplyannikov et al. 2018; Luo et al. 2019; Gharaei et al. 2018). Moreover, the conditioned medium of MSC cultures induces the migration of fibroblasts, keratinocytes, and endothelial cells and promotes the formation of capillary-like structures by HUVECs (Pereira et al. 2016).

In combined cell therapy, we critically consider the delivery methods of cells aside from the selection of cell

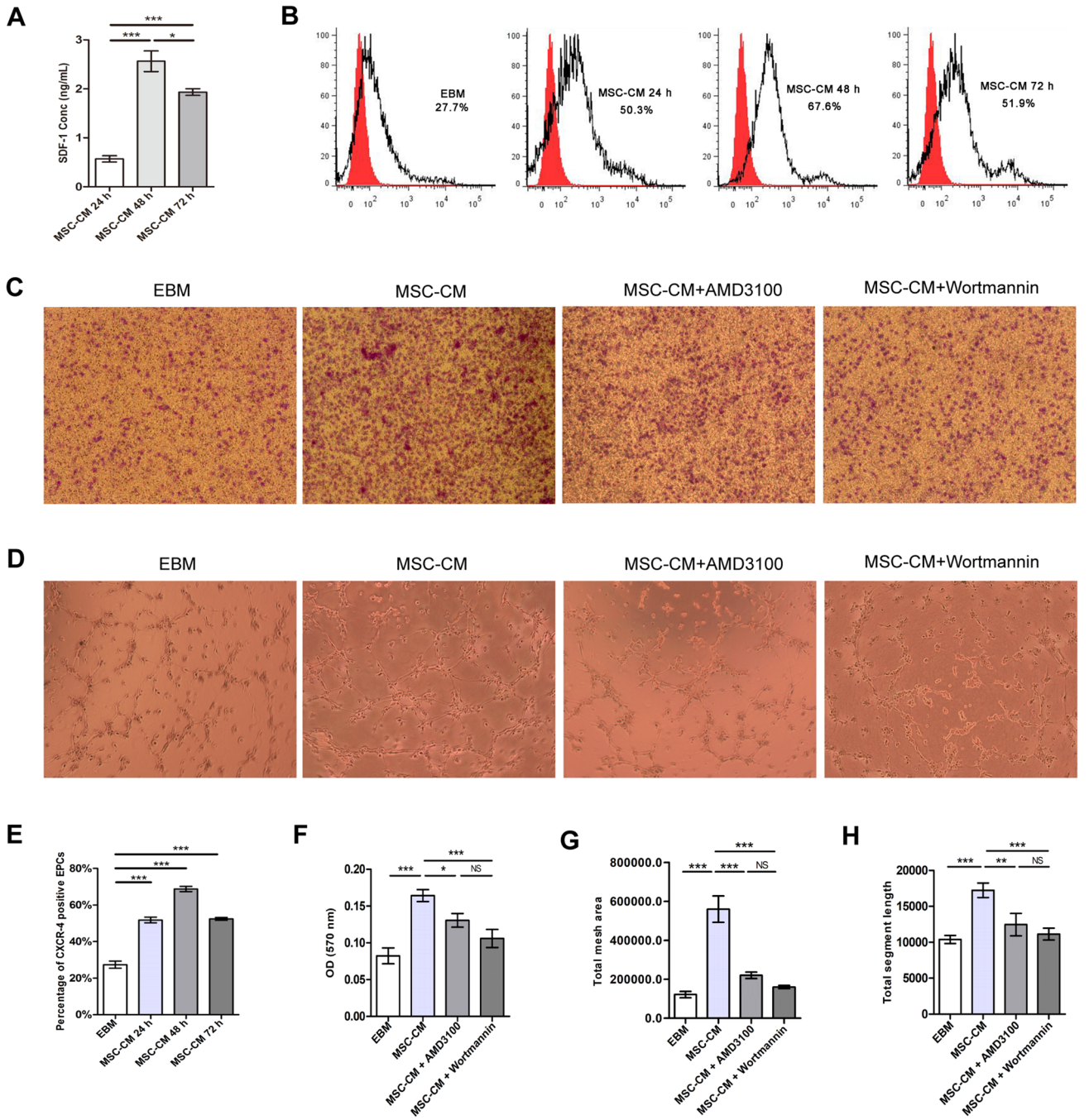

Fig. 3 The identification of EPC migration, which was contributed by MSC-secreted SDF-1 via CXCR4/PI3K/AKT signaling pathway. **a** Levels of SDF-1 secreted by MSCs at 24 h, 48 h and 72 h. **b** Representative flow cytometric analysis of CXCR4 expression (blank space) from EPCs; red space represents isotype controls. **c** Quantification analysis of CXCR4-positive EPCs induced by MSC-CM. Each experiment was repeated thrice. **d** EPCs that migrated to the subsurface of the inserts (n = 3). Scale bar, 200 μm. **e** Quantification analysis of migrating EPCs. Three independent trials were performed. **f** Tube-like structures formed by EPCs (n = 3). Scale bar, 200 μm. **g** Quantification of total mesh area and total segment length in the tube-like structure. The experiment was repeated thrice. $*p < 0.05$, $**p < 0.01$, $***p < 0.001$

types. To maximize the local concentration of EPCs in the ischemic area and increase cell invasion, we chose to implement a "dual-administration" approach, which was developed by Franz and Bartsch to treat patients with arterial occlusive disease (Franz et al. 2009, 2015; Bartsch et al. 2007). In this approach of the present study, intramuscular MSC injections were supplemented with intravenous EPC injections in contrast to previous works

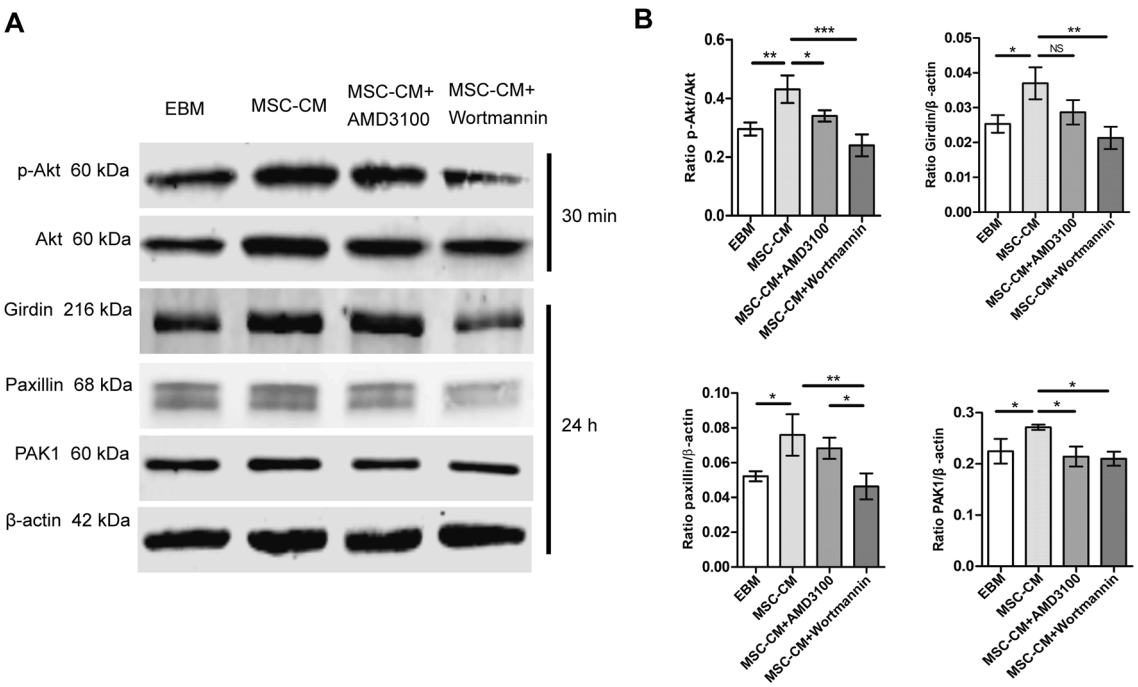

Fig. 4 Role of the AKT pathway in MSC-secreted SDF-1 induction of EPC migration. **a** AKT and phosphor-AKT levels in EPCs cultured for 30 min (top) and the levels of Girdin, Paxillin, PAK1 and β-actin in EPCs cultured for 48 h (below) in the indicated groups. **b** Bar graphs show the ratio of the densitometry measurement of phosphor-AKT to that of AKT and the ratio of the densitometry measurement of Girdin, Paxillin, PAK1 to that of β-actin. Data were obtained from three independent experiments. $*p<0.05$, $**p<0.01$, $***p<0.001$, ^{NS}no significance

in which the subjects received a mixture of MSCs and EPCs (Rossi et al. 2017; Traktuev et al. 2009). The theoretical foundation of the design is that cytokines are the crucial stimulating factor for stem cell homing, and they build an attractive gradient, with forming migratory route and guiding EPC migration to the region to be vascularized (Schmidt et al. 2007). To generate as many chemoattractants as possible, we envisioned that a vast array of chemoattractants secreted by intramuscular-administrated MSCs were locally deposited in ischemic muscle, attracting the homing of intravenous-administrated EPCs. Our results showed that Qdot® 525 labeled-EPCs in vasculature increased, and vessel numbers also increased when the combination of MSCs and EPCs was infused into the hind limb of ischemic mice. Thus, we conclude that chemoattractants secreted by MSCs promote EPC migration to the neovascularization sites.

We explored the molecular mechanism involved in EPC migration via in vitro experiments. Previous studies have suggested that SDF-1 induces EPC migration after binding to CXCR4, which is highly expressed on EPCs (Walter et al. 2005; Chiang et al. 2015). In the present work, SDF-1 concentration increased in MSC culture supernatants of different time spans. In addition, the level of CXCR4 protein in EPCs increased after incubation in MSC-CM. The data indicated that SDF-1 produced by MSCs promoted CXCR4 expression in EPCs.

AKT, a multifunctional serine/threonine protein kinase, is the downstream of class I PI3K and various receptors. PI3K-AKT signaling pathway also has a crucial effect on multiple processes, including cell proliferation, cell survival, cell migration, activation of integrins, MMP, and angiogenesis. Using both chemical inhibitors to detect the role of PI3K/AKT signaling, we found that CXCR4 and PI3K participated in EPC migration. Furthermore, AKT phosphorylation resulted in cytoskeleton changes in many cells (Chen et al. 2013). In the present study, AKT phosphorylation induced by MSC-CM was inhibited by both AMD3100 and wortmannin, indicating that phospho-AKT is the downstream of SDF-1/CXCR4/PI3K. Consistent with our results, Yu et al. revealed that SDF-1/CXCR4 mediated the migration of BMSCs toward heart MI through the activation of PI3K/AKT (Xiu et al. 2020). Dimova et al. reported that SDF-1 treatment of cardiac stem/progenitor cells increased AKT phosphorylation (Dimova et al. 2014).

Conclusion

Taken together, we argue that in combined cell therapy, MSCs facilitate the migration of circulating EPCs to neovascularization sites via the SDF-1/CXCR4/PI3K/AKT signaling pathway. Herein, we provide new insights into the mechanisms underlying the effects of combined cell therapy. These novel findings suggest that the modulation of the homing mechanism may be used as a therapeutic strategy to improve the efficacy of stem cell therapy.

Author contributions XWW and XC: conceived and designed the experiments. XYW: wrote the manuscript. ZZ and HH: cultured MSCs and EPCs, and critically revised the manuscript. XYW, HJ: performed the establishment of the mouse model of hind limb ischemia. LG and QZ: performed immunohistochemistry and immunofluorescence staining, analysed the data. LW and LX: prepared MSC-CM, performed flow cytometry and analysed the data. SW: performed the migration assay and analysed the data. WC: performed tube-like structure formation assay and analysed the data. XY: performed western blot assay and analysed the data. All the authors read and approved the final version of the manuscript.

Funding This work was supported by grants from the National Natural Science Foundation of China (No. 81760570, No. 81760371, No. 81703174) and the Project of Young and Middle-aged Scientific and Technological Innovation Leaders in Bingtuan (2018CB017) and the Autonomous Region Graduate Student Scientific Research Innovation Project (XJ2019G081).

Declarations

Conflict of interest All authors declare that they have no conflict of interest.

Ethical approval All mice were conducted in accordance with the Xinjiang Medical University Guide for Laboratory Animals and approved by the Shihezi University Ethics Committee.

References

Barsotti MC, Di Stefano R, Spontoni P, Chimenti D, Balbarini A (2009) Role of endothelial progenitor cell mobilization after percutaneous angioplasty procedure. Curr Pharm Des 15:1107–1122. https://doi.org/10.2174/138161209787846928

Bartsch T, Brehm M, Zeus T, Kögler G, Wernet P, Strauer BE (2007) Transplantation of autologous mononuclear bone marrow stem cells in patients with peripheral arterial disease (the TAM-PAD study). Clin Res Cardiol 96:891–899. https://doi.org/10.1007/s00392-007-0569-x

Chen J, Crawford R, Chen C, Xiao Y (2013) The key regulatory roles of the PI3K/AKT signaling pathway in the functionalities of mesenchymal stem cells and applications in tissue regeneration. Tissue Eng Part B Rev 19:516–528. https://doi.org/10.1089/ten.teb.2012.0672

Chiang KH, Cheng WL, Shih CM, Lin YW, Tsao NW, Kao YT (2015) Statins, HMG-CoA reductase inhibitors, improve neovascularization by increasing the expression density of CXCR4 in endothelial progenitor cells. PLoS ONE 10:e0136405. https://doi.org/10.1371/journal.pone.0136405

Chong MSK, Ng WK, Chan JKY (2016) Concise review: endothelial progenitor cells in regenerative medicine: applications and challenges. Stem Cells Transl Med 5:530–538. https://doi.org/10.5966/sctm.2015-0227

Couffinhal T, Silver M, Zheng LP, Kearney M, Witzenbichler B, Isner JM (1998) Mouse model of angiogenesis. Am J Pathol 152:1667–1679

Dimova N, Wysoczynski M, Rokosh G (2014) Stromal cell derived factor-1a promotes c-kit^{+} cardiac stem/progenitor cell quiescence through casein kinase 1α and GSK3β. Stem Cells 32:487–499. https://doi.org/10.1002/stem.1534

Franz RW, Parks A, Shah KJ, Hankins T, Hartman JF, Wright ML (2009) Use of autologous bone marrow mononuclear cell implantation therapy as a limb salvage procedure in patients with severe peripheral arterial disease. J Vasc Surg 50:1378–1390. https://doi.org/10.1016/j.jvs.2009.07.113

Franz RW, Shah KJ, Pin RH, Hankins T, Hartman JF, Wright ML (2015) Autologous bone marrow mononuclear cell implantation therapy is an effective limb salvage strategy for patients with severe peripheral arterial disease. J Vasc Surg 62:673–680. https://doi.org/10.1016/j.jvs.2015.02.059

Ghadge SK, Mühlstedt S, Bader ÖC (2011) SDF-1α as a therapeutic stem cell homing factor in myocardial infarction. Pharmacol Ther 129:97–108. https://doi.org/10.1016/j.pharmthera.2010.09.011

Gharaei MA, Xue Y, Mustafa K, Lie SA, Fristad I (2018) Human dental pulp stromal cell conditioned medium alters endothelial cell behavior. Stem Cell Res Ther 9:69. https://doi.org/10.1186/s13287-018-0815-3

Han Y, Li X, Zhang Y, Han Y, Chang F, Ding J (2019) Mesenchymal stem cells for regenerative medicine. Cells 8(8):1–32. https://doi.org/10.3390/cells8080886

Konoplyannikov M, Kotova S, Baklaushev V, Konoplyannikov A, Kalsin V, Timashev P, Troitskiy A (2018) Mesenchymal stem cell therapy for ischemic heart disease: advances and challenges. Curr Pharm Des 24(26):3132–3142. https://doi.org/10.2174/1381612824666180913151059

Lasala GP, Silva JA, Gardner PA, Minguell JJ (2010) Combination stem cell therapy for the treatment of severe limb ischemia: safety and efficacy analysis. Angiology 61:551–556. https://doi.org/10.1177/0003319710364213

Lasala GP, Silva JA, Kusnick BA, Minguell JJ (2011) Combination stem cell therapy for the treatment of medically refractory coronary ischemia: A Phase I study. Cardiovasc Revasc Med 12:29–34. https://doi.org/10.1016/j.carrev.2010.01.001

Lasala GP, Silva JA, Minguell JJ (2012) Therapeutic angiogenesis in patients with severe limb ischemia by transplantation of a combination stem cell product. J Thorac Cardiovasc Surg 144:377–382. https://doi.org/10.1016/j.jtcvs.2011.08.053

Li YN, Chang S, Li WL, Tang GH, Ma YY, Liu YQ, Yuan F, Zhang ZJ, Yang GY, Wang YT (2018) cxcl12-engineering endothelial progenitor cells enhance neurogenesis and angiogenesis after ischemic brain injury in mice. Stem Cell Res Ther 9(1):139–153. https://doi.org/10.1186/s13287-018-08656

Luo R, Lu Y, Liu J, Cheng J, Chen Y (2019) Enhancement of the efficacy of mesenchymal stem cells in the treatment of ischemic diseases. Biomed Pharmacother 109:2022–2034. https://doi.org/10.1016/j.biopha.2018.11.068

Medina RJ, Barber CL, Sabatier F, Dignat-George F, Melero-Martin JM, Khosrotehrani K, Ohneda O, Randi AM, Chan JKY, Yamaguchi T, Van Hinsbergh VWM, Yoder MC, Stitt AW (2017) Endothelial progenitors: a consensus statement on nomenclature. Stem Cells Transl Med 6:1316–2130. https://doi.org/10.1002/sctm.16-0360

Niiyama H, Huang NF, Rollins MD, Cooke JP (2009) Murine model of hindlimb ischemia. J vis Exp 23:1035. https://doi.org/10.3791/1035

Pereira ARS, Mendes TF, Ministro A, Teixeira M, Filipe M, Santos JM, Bárcia RN, Goyri-O'Neill J, Pinto F, Cruz PE, Cruz HJ, Santos SCR (2016) Therapeutic angiogenesis induced by human umbilical cord tissue-derived mesenchymal stromal cells in a murine model of hindlimb ischemia. Stem Cell Res Ther 7:145. https://doi.org/10.1186/s13287-016-0410-4

Rossi E, Smadja D, Goyard C, Cras A, Dizier B, Bacha N, Lokajczyk A, Guerin CL, Gendron N, Planquette B, Mignon V, Bernabéu C, Sanchez O, Smadja DM (2017) Co-injection of mesenchymal stem cells with endothelial progenitor cells accelerates muscle recovery in hind limb ischemia through an endoglin-dependent mechanism. Thromb Haemost 117:1908–1918. https://doi.org/10.1160/TH17-01-0007

Schmidt A, Brixius K, Bloch W (2007) Endothelial precursor cell migration during vasculogenesis. Circ Res 101:125–136. https://doi.org/10.1161/CIRCRESAHA.107.148932

Sun Y, Feng Y, Zhang CQ, Cheng XG, Chen SB, Ai ZS, Zeng BF (2011) Beneficial effect of autologous transplantation of endothelial progenitor cells on steroid-induced femoral head osteonecrosis in rabbits. Cell Transplant 20:233–243. https://doi.org/10.3727/096368910X522234

Teranishi F, Takahashi N, Gao N, Akamo Y, Takeyama H, Manabe T, Okamoto T (2009) Phosphoinositide 3-kinase inhibitor (wortmannin) inhibits pancreatic cancer cell motility and migration induced by hyaluronan in vitro and peritoneal metastasis in vivo. Cancer Sci 100:770–777. https://doi.org/10.1111/j.1349-7006.2009.01084.x

Traktuev DO, Prater DN, Merfeld-Clauss S, Sanjeevaiah AR, Saadatzadeh MR, Murphy M, Johnstone BH, Ingram DA, March KL (2009) Robust functional vascular network formation in vivo by cooperation of adipose progenitor and endothelial cells. Circ Res 104:1410–1420. https://doi.org/10.1161/CIRCRESAHA.108.190926

Tsai FC, Seki A, Yang HW, Hayer A, Carrasco S, Malmersjö S, Meyer T (2014) A polarized Ca2+, diacylglycerol and STIM1 signalling system regulates directed cell migration. Nat Cell Biol 16:133–144. https://doi.org/10.1038/ncb2906

Vanden Berg-Foels WS (2014) In situ tissue regeneration: chemoattractants for endogenous stem cell recruitment. Tissue Eng Part B Rev 20:28–39. https://doi.org/10.1089/ten.TEB.2013.0100

Walter DH, Haendeler J, Reinhold J, Rochwalsky U, Seeger F, Honold J, Hoffmann J, Urbich C, Lehmann R, Arenzana-Seisdesdos F, Aicher A, Heeschen C, Fichtlscherer S, Zeiher AM, Dimmeler S (2005) Impaired CXCR4 signaling contributes to the reduced neovascularization capacity of endothelial progenitor cells from patients with coronary artery disease. Circ Res 97:1142–1151. https://doi.org/10.1161/01.RES.0000193596.94936.2c

Wang XY, Zhao ZS, Zhang HW, Hou JX, Feng WL, Zhang M, Guo J, Xia J, Ge QH, Chen XL, Wu XW (2018) Simultaneous isolation of mesenchymal stem cells and endothelial progenitor cells derived from murine bone marrow. Exp Ther Med 16:5171–5177. https://doi.org/10.3892/etm.2018.6844

Xiu G, Li X, Yin Y, Li J, Li B, Chen X, Liu P, Sun J, Ling B (2020) SDF-1/CXCR4 Augments the therapeutic effect of bone marrow mesenchymal stem cells in the treatment of lipopolysaccharide-induced liver injury by promoting their migration through PI3K/AKT signaling pathway. Cell Transplant 29:1–12. https://doi.org/10.1177/0963689720929992

Xue YJ, Zhou BD, Wu J, Miao GB, Li K, Li SY, Zhou J, Geng Y, Zhang P (2020) Transplantation of endothelial progenitor cells in the treatment of coronary artery microembolism in rats. Cell Transplant 29:1–8. https://doi.org/10.1177/0963689720912688

Yong KW, Choi JR, Mohammadi M, Mitha AP, Sanati-Nezhad A, Sen A (2018) Mesenchymal stem cell therapy for ischemic tissues. Stem Cells Int 2018:1–11. https://doi.org/10.1155/2018/8179075

Yu Q, Liu LZ, Lin J, Wang Y, Xuan X, Guo Y, Hu S (2015) SDF-1α/CXCR4 axis mediates the migration of mesenchymal stem cells to the hypoxic-ischemic brain lesion in a rat model. Cell J 16:440–447. https://doi.org/10.22074/cellj.2015.504